Chapter

Review of Mathematical Models for the Anaerobic Digestion Process

Borja Velázquez-Martí, Orlando W. Meneses-Quelal, Juan Gaibor-Chavez and Zulay Niño-Ruiz

Abstract

To describe anaerobic fermentation, many mathematical models have been suggested. A commonly accepted hypothesis in microbial growth is the speed of cellular reproduction, which is proportional to the concentration of cells at that instant. The constant of proportionality between the speed of growth and cell concentration is called cell growth rate, μ. In many occasions, the cell growth rate is considered constant. This leads to conclude that the concentration of cells versus time presents an exponential function. The consideration of this equation provides a good adjustment in the beginning of central phase of the anaerobic fermentation process. However, it moves away from the measurements when there is a limited reproduction due to lack of nutrients and competition between the cells in the environment. This produces a sigmoidal variation in concentration. To find a suitable fit function for all phases of the process, Gompertz proposes a model that considers the cell growth rate as variable. In this chapter, the Gompertz model, kinetic models, transference, and cone models are evaluated. Different adaptations to fit the variables to the obtained values in the experiments have been reviewed.

Keywords: mathematical model, Gompertz, fermentation, kinetic model, methane

1. Introduction

Anaerobic digestion is a biological process in which the organic matter in the absence of oxygen, and through the action of a group of specific bacteria, is broken down into a set of gaseous products, called biogas, formed by CH_4, CO_2, H_2, H_2S, etc. and in a digestate, which is a mixture of mineral substances (N, P, K, Ca, etc.) and compounds of difficult degradation [1]. One of the objectives of anaerobic digestion is the production of methane, which can be used as fuel. Anaerobic digestion is considered one of the most important and advantageous processes in the treatment of livestock manure and sludge residues. It represents a possibility to reduce its environmental impact while at the same time, providing a biofuel for local energy needs [2]. This process has been known for hundreds of years; however, it is still the object of research due to the great variability of the conditions in which it can be produced, diversity of raw materials, and influential factors.

Table 1 shows some of the most recent researches. In recent years, there has been an increasing interest in new raw fermentation materials, mainly

Author	Material	Pretreatment	Methane potential m^3 $kg^{-1}SV$
Bayrakdar et al. [4]	Chicken manure		0.272
Franco et al. [5]	Wheat straw + inoculum		0.229
Franco et al. [5]	Wheat straw + glucose + ac. Formic + inoculum*		0.276
Guo et al. [6]	Excessively withered corn straw + glucose		0.282
Li et al. [7]	Parton + sheep manure		0.152
Li et al. [7]	Paper + sheep manure		0.199
Mancini et al. [8]	Lignocellulose in general	N-methylmorpholine N-oxide	0.304
Martín Juárez et al. [9]	Microalgae + pig manure	Alkaline pretreatment with NAOH	0.377
Mustafa et al. [10]	Bagasse of sugarcane + inoculum*	Hydrothermal pretreatment	0.318
Vazifehkhoran et al. [11]	Wheat straw + sewage		0.314
Xu et al. [12]	Corn straw + *Bacillus Subtilis*	Microaerobic mesolithic	0.270
Zahan et al. [13]	*Gallinaza* (sawdust, wood shavings, and rice or straw husk) with yogurt serum		0.670
Aboudi et al. [14]	Dry sediment of sugar beet tails + pig manure		0.260
Dennehy et al. [15]	Food waste and pig manure		0.521
Glanpracha and Annachhatre [16]	Cassava pulp with pig manure		0.380
Marin Batista et al. [17]	Vinasse and chicken manure (chicken dung)		0.650
Aboudi et al. [18]	Dry beet granules of sugar beet + cow dung		0.280
Belle et al. [19]	Fodder radish with cow dung		0.200
Cestonaro et al. [20]	Sheep litter (mixture of rice husk with feces and urine) + cattle manure		0.171
Di Maria et al. [21]	Sludge from wastewater with fruit and vegetable waste		0.216
Fu et al. [22]	Corn straw + inoculum *	Thermophilic microaerobic	0.326
Fu et al. [23]	Corn straw + inoculum *	Secondary thermophilic microaerobic	0.381
Agyeman and Tao [24]	Food waste + livestock manure		0.467

**Inoculum is material obtained from the effluent of a previous biogas plant that ferments raw materials, such as manure from pigs, cows, sheep, chickens, and other animals, at mesophilic ranges.*

Table 1.
Values obtained from methane potential in various co-digestion processes.

lignocellulosic materials from agriculture, or waste such as paper and cardboard. So, co-digestion processes are being analyzed, which consist of improving methane production by mixing materials that ferment better together than separated due to the enriched microbial load; in this way, their nutritional needs are better complemented.

New inocula, such as the rumen, and its interaction with the raw material are also being examined, together with nutritional requirements. Pretreatment studies are being carried out along with thermal sequences in the processes, alternating thermophilic and mesophilic stages and evaluating the productivity, kinetics, and net energy balance. The microbiological identification involved in the fermentation according to the substrate and the followed thermal process also acquire interest.

One of the most discussed aspects is mathematical modeling. The objective of the modeling is to be able to establish characteristic parameters of the raw material and process conditions to predict the system's evolution over time, the performance obtained, and fermentation speed. In this study the most important models are evaluated.

Anaerobic digestion comprises a decomposition mechanism of organic matter based on three stages [3]: first a hydrolytic phase, in which polymers of long carbon chains are broken obtaining shorter acid chains, subsequently, an acetogenic phase, in which the short-chain acids obtained in the previous phase are transformed into acetic acid, and finally, a methanogenic phase, in which the acetic acid is transformed into methane.

Each of these stages is provided by a differentiated microbiological group. Each group takes as a substrate to the product generated in the previous phase. When the evolution of a microbial group is analyzed in a batch-type reactor, in batches, the variation of cell concentration varies, as shown in **Figure 1**.

Initially, the concentration of microorganisms responsible of digestion is small and evolves very slowly in this stage because it needs time to adapt. This phase is called *lag phase*, or lethargy. Subsequently, there is a very rapid increase in cell concentration called the growth phase. The growth phase ends when cell compete for substrate, causing a number of cell replications to equal deaths, so the number of living cells is stabilized. This phase is called the *stationary phase*. The stationary

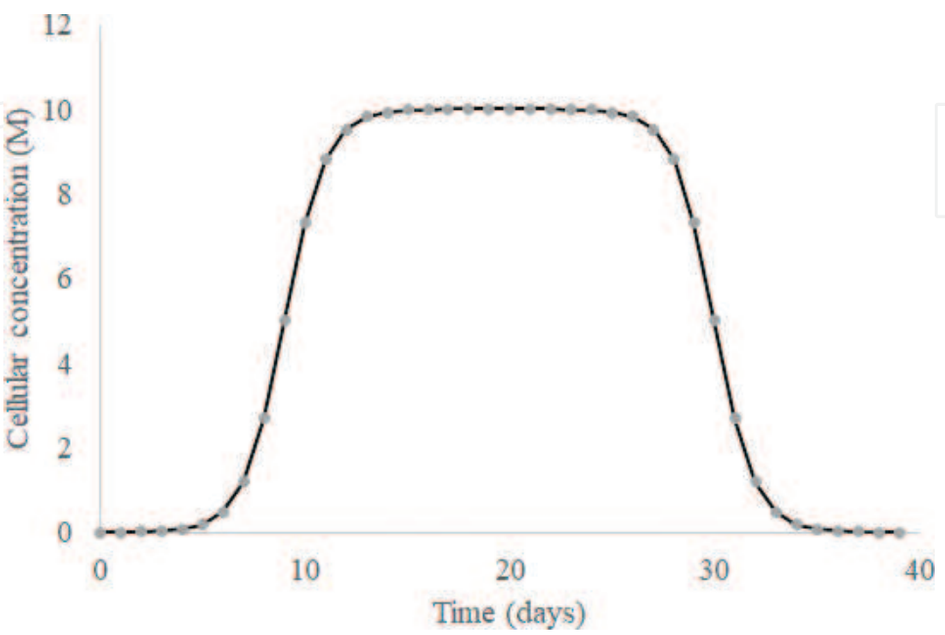

Figure 1.
Variation of cell concentration over time in a batch reactor.

phase ends when this battle for substrate causes a higher number of deaths than the number of reproductions, resulting in cell concentration to fall sharply. This phase is called the cell *death phase*.

From the practical point of view, it is only interesting to analyze the period between the beginnings of the fermentation to the stationary phase, appearing a curve similar to the sigmoid one. However, the sigmoid equation does not correctly fit the experimental results obtained.

2. Exponential model

A model widely used to describe the variation of cell concentration in the growth phase has been the exponential model. This model is based on the hypothesis that the speed of growth in an instant is proportional to the concentration of cells existing at that moment. This is expressed mathematically by Eq. (1), where X is the concentration of cells and μ is the constant of proportionality called cell growth rate:

$$\frac{dX}{dt} = \mu \cdot X \tag{1}$$

The development of Eq. (1) shows that, in the growth phase, the variation of cells follows an exponential curve:

$$\frac{dX}{X} = \mu \cdot dt$$

$$\int_{X_1}^{X_2} \frac{dX}{X} = \int_{t_{lag}}^{t} \mu \cdot dt$$

$$\ln \frac{X_2}{X_1} = \mu \cdot \left(t - t_{lag}\right)$$

$$X_2 = X \cdot {}_1e^{\mu \cdot \left(t - t_{lag}\right)}$$

t_{lag} is the lag time. The cell growth rate has as unit the inverse of time (d^{-1}) and can be calculated experimentally with Eq. (2):

$$\mu = \frac{X_2 - X_1}{X_1 \cdot \left(t - t_{lag}\right)} \tag{2}$$

This model is not completely satisfactory because it has been verified that μ is not constant and it varies as time goes by. As competition for the substrate increases, the curve in **Figure 1** moves away from the exponential. To achieve a better fit, Monod proposed a model for calculating the cell growth rate as a function of the substrate concentration according to Eq. (3), where S is the substrate concentration at a given time, $\mu_{\max}$ is the maximum rate of cell growth, and Ks is a constant called saturation:

$$\mu = \frac{\mu_{\max} \cdot S}{K_s + S} \tag{3}$$

The Monod model proposes the existence of a maximum cell growth rate and a saturation constant that are characteristics of microbial species growing under

defined conditions. The maximum growth rate is the one that occurs initially in the growth phase exponentially. When the substrate begins to be scarce, the rate decreases with respect to the maximum.

Along with the Monod model, there are others with the same style that can be observed in **Table 2**. In all of them, it can be seen that the maximum rate value considered in the exponential phase is minorized when the substrate concentration is low.

The relationship between the variations of cell concentration is always proportional to substrate consumption. The proportionality constant is called the biomass/substrate yield $Y_{x/s}$ and is defined by Eq. (4), where S_0 and S_1 are the initial and final substrate concentrations and X_0 and X_1 are the initial and final cell concentrations:

$$Y_{x/s} = \frac{X_1 - X_0}{S_0 - S_1} \tag{4}$$

If the initial concentration of substrate (So) is known, the variation of cell mass during the process is obtained from the biomass/substrate ratio of the process *Yx/s*. Limiting the decrease in the growth rate to a certain percentage of its maximum value allows calculating the time retention (*TR*) in a bioreactor batch.

$$z \cdot \mu_{\max} = \frac{\mu_{\max} S_1}{K_s + S_1} (0<z<1) \rightarrow S_1 = \frac{z}{1-z} \cdot K_s$$

$$Y_{x/s} = \frac{X_1 - X_0}{S_0 - S_1} \rightarrow X_1 = X_0 + Y_{x/s} \cdot (S_0 - S_1)$$

$$\ln \frac{X_1}{X_o} = \mu_{\max} \cdot \left(TR - t_{lag}\right) \rightarrow TR = t_{lag} + \frac{1}{\mu_{\max}} \ln \frac{X_1}{X_o}$$

The amount of product generated per unit volume and time (*P*) and methane in this case (*M*) are proportional to the variation of cell concentration (*X*). The proportionality constant $Y_{p/x}$ is called product/biomass yield:

$$Y_{p/x} = \frac{P_1 - P_0}{X_1 - X_0}$$

Type of model	Author	Model
Kinetic models without inhibition	Tessier	$\mu = \mu_{\max} \cdot \left(1 - e^{-S/K_s}\right)$
	Moser	$\mu = \mu_{\max} \frac{S^n}{K_s \cdot a + S^n}$
	Contois	$\mu = \mu_{\max} \frac{S}{BX + S}$
Kinetic models with inhibition	Andrews and Noak	$\mu = \mu_{\max} \frac{1}{K_s + S + \frac{S^2}{K_{is}}}$
	Webb	$\mu = \mu_{\max} \frac{S \cdot \left(1 + \frac{\beta \cdot S}{K_{is}}\right)}{K_s + S + \frac{S^2}{K_{is}}}$
	Aiba et al.	$\mu = \mu_{\max} \frac{S}{K_s + S} e^{-S/K_{si}}$
	Teissier	$\mu = \mu_{\max} \left[e^{-S/K_{si}} - e^{-S/K_s}\right]$
	Tseng and Wymann	$\mu = \mu_{\max} \frac{S}{K_s + S} - K_{si}(s - s_c)$

Table 2.
Variation models of the cell growth rate [25].

$$\frac{dM}{dt} = Y_{p/x} \cdot \frac{dX}{dt}$$

Since the variation of cell concentration is proportional to the concentration of cells at a given time, we have to.

$$\frac{dM}{dt} = Y_{p/s} \cdot \mu X$$

By developing the variation of cell concentration over time, it has been demonstrated that the amount of product obtained (methane) follows an exponential growth during the exponential growth of microorganisms. That is the reason because working in this phase with batch-type bioreactors is preferred for optimum performance. To do this, you must adjust the retention time to the duration of this stage.

X_0 represents the initial cell concentration in the reactor; X represents cell concentration at a time t, *and* t_{lag} is the time of lethargy or cellular adaptation:

$$\frac{dM}{dt} = Y_{p/s} \cdot \mu X_0 \cdot e^{\mu(t-tlag)}$$

$$M = Y_{p/s} \cdot X_0 \cdot \left(e^{\mu(t-tlag)} - 1\right)$$

whereas the value of $Y_{p/s} \cdot X_0$ is negligible compared to the exponential, that is $Y_{p/s} \cdot X_0 <<< Y_{p/s} \cdot X_0 \cdot e^{\mu(t-tlag)}$, the accumulated volume obtained in each experiment can be graphically represented with the model of Eq. (1), calculating the cell growth rate, the productivity of the substrate, and the optimum retention time for a greater use of energy:

$$M = Y_{p/s} \cdot X_0 \cdot e^{\mu(t-tlag)}$$

3. Model of Gompertz

Despite the practicality of the exponential model when complemented by the Monod equation, it is not completely satisfactory because it does not describe well the variation of cell concentration as the substrate is being consumed and the stationary phase approaches. Knowing how cell growth behaves in this area is significantly relevant if you want to use high retention times.

To find an adequate adjustment function for all phases of the process, Winsor [26] proposes to use an equation developed by Gompertz [27] in human demography. This proposes a model that considers the variable cell growth rate, as shown in Eqs. (5) and (6), where a and c are constants:

$$\frac{dX}{dt} = c \cdot \ln(a/X) \cdot X \quad (5)$$

$$\mu = c \cdot \ln(a/X) \quad (6)$$

According to Eq. (6), Gompertz moves radically away from the Monod approach, since the cell growth rate has no maximum. If there was a maximum, the derivative of Eq. (6) would be canceled at some point, something that does not happen:

$$\lim_{X\to 0}\mu = \lim_{X\to 0} c\cdot \ln\left(a/X\right) = \infty$$

$$\lim_{X\to \infty}\mu = \lim_{X\to \infty} c\cdot \ln\left(a/X\right) = -\infty$$

$$\frac{d\mu}{dt} = c\frac{X}{a}\cdot\left(\frac{-a}{X^2}\right) = \frac{-c}{X}$$

To obtain the function of cell concentration in time according to Gompertz, we must solve Eq. (5), which is a differential equation of separable variables:

$$\frac{dX}{X\cdot \ln\left(a/X\right)} = c\cdot dt$$

$$\int_{X0}^{X}\frac{dX}{X\cdot \ln\left(a/X\right)} = \int_0^t c\cdot dt$$

$$-\left[\ln\left(\ln\frac{a}{X}\right) - \ln\left(\ln\frac{a}{X_0}\right)\right] = ct$$

$$\ln\left(\frac{\ln\frac{a}{X_0}}{\ln\frac{a}{X}}\right) = ct$$

$$\frac{\ln\frac{a}{X_0}}{e^{ct}} = \ln\frac{a}{X}$$

Since a and X_0 are constants, the following consideration can be made:

$$\ln\frac{a}{X_0} = B = e^b$$

$$e^{e^{-ct+b}} = \frac{a}{X_0}$$

Therefore, Eq. (7) is obtained, which describes the cellular concentration in the reactor for each instant. This equation is the true contribution of the Gompertz:

$$X = a\cdot e^{\left[-e^{-ct+b}\right]} \tag{7}$$

When analyzing the limits in zero and infinity, we observe that the initial concentration of cells is *X1* and that a represents an asymptote corresponding to the maximum cell potential, which would occur in the steady state:

$$\lim_{t\to 0} X = a\cdot e^{-B} = a\cdot e^{\ln\frac{X_0}{a}} = X_0$$

$$\lim_{t\to \infty} X = a$$

3.1 Considerations to the Gompertz model

If we accept the Gompertz model, Zwietering et al. [28] suggest modifications providing physical meaning to these variables. The rate of growth can be redefined as Eq. (8):

$$\frac{dX}{dt} = a\cdot e^{\left[-e^{-ct+b}\right]}\cdot\left(-e^{-ct+b}\right)\cdot -c = a\cdot c\cdot e^{\left[-e^{-ct+b}\right]}\cdot e^{-ct+b}$$

$$\frac{dX}{dt} = a \cdot c \cdot e^{\left[-e^{-ct+b}\right]} \cdot e^{-ct+b} \tag{8}$$

The instant in which the maximum growth velocity t_m occurs would be calculated from the first derivative of the velocity equal to zero, which is the same as the second derivative of the Gompertz Eq. (7). This implies that at that point where the growth speed is at maximum, the Gompertz function has a turning point:

$$\frac{d^2X}{dt^2} = a \cdot c^2 \cdot e^{\left[-e^{-ct+b}\right]} \cdot \left(e^{-ct+b}\right)^2 - a \cdot c^2 \cdot e^{\left[-e^{-ct+b}\right]} \cdot \left(e^{-ct+b}\right)$$

$$\frac{d^2X}{dt^2} = a \cdot c^2 \cdot e^{\left[-e^{-ct+b}\right]} \cdot \left(e^{-ct+b}\right) \cdot \left[\left(e^{-ct+b}\right) - 1\right]$$

$$\frac{d^2X}{dt^2} = a \cdot c^2 \cdot e^{\left[-e^{-ct_m+b}\right]} \cdot \left(e^{-ct_m+b}\right) \cdot \left[\left(e^{-ct_m+b}\right) - 1\right] = 0$$

$$-ct_m + b = 0$$

$$t_m = \frac{b}{c}$$

The concentration of cells where the maximum reproduction speed occurs is calculated by entering the value of t_m in Eq. (7), and it is shown that the growth rate where the reproduction speed is at maximum equals c:

$$X = a \cdot e^{\left[-e^{-ct_m+b}\right]} = a \cdot e^{\left[-e^{-c\frac{b}{c}+b}\right]} = \frac{a}{e}$$

$$\mu_m = c \cdot \ln\left(a/(a/e)\right) = c$$

The maximum reproduction speed value is obtained by substituting t_m in Eq. (8):

$$v_{\max} = \frac{dX_{tm}}{dt} = a \cdot c \cdot e^{\left[-e^{-ct_m+b}\right]} \cdot e^{-ct+b} = a \cdot c \cdot e^{\left[-e^{-c\frac{b}{c}+b}\right]} \cdot e^{-c\frac{b}{c}+b} = \frac{a \cdot c}{e}$$

According to the previous thing, the curve tangent X in the point of inflection t_m has the form:

$$X = \frac{a \cdot c}{e} t + k$$

$$\text{Given the } t = t_m = \frac{b}{c} \text{ y } X_{tm} = \frac{a}{e,} \text{ so :}$$

$$\frac{a}{e} = \frac{a \cdot c}{e} \cdot \frac{b}{c} + k \rightarrow k = \frac{a}{e} - \frac{a \cdot b}{e} = \frac{a}{e}(1-b)$$

$$X = \frac{a \cdot c}{e} t + \frac{a}{e}(1-b) = \frac{a}{e} \cdot (ct + (1-b))$$

If we define the latency time, t_{lag}, as the time in which the tangent line at the curve inflection point (point that coincides with maximum velocity) cuts the axis of the abscissa, we have that the latency time is in $X = 0$:

$$0 = ct_{lag} + (1-b)$$

$$t_{lag} = \frac{(b-1)}{c}$$

From this equation, b can also be expressed as.

$$b = c \cdot t_{lag} + 1$$

$$\text{And } v_{\max} = \frac{a \cdot c}{e}, \text{ the result}$$

$$b = \frac{v_{\max} \cdot e}{a} \cdot t_{lag} + 1$$

Obtaining the Gompertz equation is Eq. (9). This equation has become popularized as the *modified Gompertz equation*:

$$X = a \cdot e^{\left[-e^{\frac{v_{\max} \cdot e}{a}\left(t_{lag}-t\right)+1}\right]} \tag{9}$$

This equation has been used in current research, such as Bah et al. [29], Capson-Tojo et al. [3], Bayrakdar et al. [4], Mancini et al. [8], Martín Juárez et al. [9], and Li et al. [7].

To experimentally obtain the maximum reproduction speed and the latency time, X is measured as well as the reactor time. Next by defining the value of a as the maximum cell concentration obtainable, Eq. (9) then can be linearized:

$$\ln\left(\ln\frac{X}{a}\right) = -\frac{v_{\max} \cdot e}{a}t + \left(1 + \frac{v_{\max} \cdot e}{a}t_{lag}\right)$$

The latency time and the maximum speed of cellular reproduction will be characteristics of the microbial group in certain conditions.

3.2 Cumulative production curve of methane applying Gompertz

If we consider the product/biomass yield, we have.

$$Y_{p/x} = \frac{P_1 - P_0}{X_1 - X_0} = \frac{dM}{dX}$$

$$\frac{dM}{dt} = Y_{p/x}\frac{dX}{dt} \tag{10}$$

$$\frac{dM}{dt} = Y_{p/x} \cdot a \cdot c \cdot e^{\left[-e^{-ct+b}\right]} \cdot e^{-ct+b}$$

$$\frac{dM}{dt} = Y_{p/x} \cdot a \cdot c \cdot e^{\left[-e^{-\frac{v_{\max} \cdot e}{a}t+\frac{v_{\max} \cdot e}{a}t_{lag}+1}\right]} \cdot e^{-\frac{v_{\max} \cdot e}{a}t+\frac{v_{\max} \cdot e}{a}t_{lag}+1}$$

$$\frac{dM}{dt} = Y_{p/x} \cdot a \cdot c \cdot e^{\left[-e^{\frac{v_{\max} \cdot e}{a}\left(t_{lag}-t\right)+1}\right]} \cdot e^{\frac{v_{\max} \cdot e}{a}\left(t_{lag}-t\right)+1}$$

$$M = \int_0^t Y_{p/x} \cdot a \cdot c \cdot e^{\left[-e^{\frac{v_{\max} \cdot e}{a}\left(t_{lag}-t\right)+1}\right]} \cdot e^{\frac{v_{\max} \cdot e}{a}\left(t_{lag}-t\right)+1}dt$$

From Eq. (10), we obtain the cumulative methane production Eq. (11):

$$M = Y_{p/x} \cdot a \cdot e^{\left[-e^{\frac{v_{\max} \cdot e}{a}\left(t_{lag}-t\right)+1}\right]} \tag{11}$$

Taking limit when the time tends to infinity, it is shown that the methane potential produced is $Y_{p/x} \cdot a$:

$$\lim_{t \to 0} M = Y_{p/x} \cdot a \cdot e^{-B} = Y_{p/x} \cdot a \cdot e^{\ln \frac{X_1}{a}} = Y_{p/x} \cdot X_0$$

$$\lim_{t \to \infty} M = Y_{p/x} \cdot a$$

If we calculate the second derivative of the methane production curve and we equate to zero, then a maximum methane speed production point occurs:

$$\frac{d^2M}{dt^2} = 0$$

$$Y_{p/x} \cdot a \cdot c \cdot e^{\left[-e^{\frac{v_{\max} \cdot e}{a}\left(t_{lag}-t\right)+1}\right]} \cdot \left(-\frac{v_{\max} \cdot e}{a}\right) \cdot e^{\frac{v_{\max} \cdot e}{a}\left(t_{lag}-t\right)+1} \cdot \left(\left(-e^{\frac{v_{\max} \cdot e}{a}\left(t_{lag}-t\right)+1}\right)+1\right) = 0$$

$$\frac{v_{\max} \cdot e}{a}\left(t_{lag}-t\right)+1 = 0$$

$$t = \frac{a}{v_{\max} \cdot e} + t_{lag} = \frac{b}{c}$$

The maximum methane production rate is $v_{CH4\max}$:

$$v_{M\max} = Y_{p/x}\frac{a \cdot c}{e}$$

Lay et al. [30] proposed to modify the Gompertz Eq. (9) by applying the potential of producible methane, $M_e = Y_{p/x} \cdot a$, expressed as Eq. (12):

$$M = M_e \cdot e^{\left[-e^{\frac{v_{M\max} \cdot e}{M_e}\left(t_{lag}-t\right)+1}\right]} \tag{12}$$

Table 1 shows the values obtained from the methane potential in various co-digestion studies. All of them were carried out in mesophilic conditions, between 30 and 37°C. It can be observed that the production of methane in most cases ranges between 0.15 and 0.65 m^3 kg^{-1}SV. Based on this calculation, we could classify the digestion processes into three groups: (a) low-production processes, the amount of methane produced is between 0.15 and 0.30 m^3 kg^{-1}SV, (b) medium-production processes, the amount of methane produced is between 0.300 and 0.45 m^3 kg^{-1}SV, and (c) high-production processes, the amount of methane produced is greater than 0.45 m^3 kg^{-1}SV.

These types of productions and their energy equivalence mean that anaerobic digestion processes are considered more as a waste management and treatment process with a complementary energy product than as an alternative energy source to the problems derived from the limitation of fossil fuels.

3.3 Conclusions of the Gompertz model

The Gompertz model provides an equation that describes cell concentration over time in a fermentation process.

To define this equation, it is necessary to obtain the value of three constants: a is the maximum cellular concentration, b is a constant that depends on the initial concentration of cells and a, and c is the value of the cell growth rate where the growth velocity is at maximum, that is, at the inflection point of the curve.

The Gompertz model implies that there is no maximum cell growth rate.

4. Kinetic models

The complexity of the Gompertz model and the problems that exist when applying the derivatives of the Monod and Contois equation have led some researchers to suggest models that do not focus on the growth rate but on the kinetics of substrate degradation or product formation. Brulé et al. [31] classify the kinetic models into four groups:

a. Reaction in a single step with first-order kinetics.

b. Two-step reaction with first-order kinetics.

c. Reaction in two speeds of a single step with first-order kinetics.

d. Reaction in two speeds of two steps with first-order kinetics.

4.1 One-step reaction with first-order kinetics

This model shows reaction rate is proportional to the amount of reagent, in this case substrate. So

$$\frac{dS}{dt} = k \cdot S \rightarrow S = S_0 \cdot e^{-k \cdot t}$$

where S is the amount of substrate at a time t, S_0 is the initial substrate amount, and k is the kinetic constant.

As the mass in the reaction is conserved, the mass of product M (methane) is calculated as

$$M = S_0 \cdot \left(1 - e^{-k \cdot t}\right)$$

Angelidaki et al. [32] used this kinetic type, relating the concentration of methane that is generated in a reactor with the maximum potential through the following equation:

$$\ln\left(\frac{M_e - M}{M_e}\right) = -k \cdot t$$

$$M = M_e \cdot \left(1 - e^{-k \cdot t}\right)$$

where M is the methane produced at a given time t, M_e is the value of the final methane production, and k is the constant of the hydrolysis rate.

Díaz et al. [33] evaluated the digestion of cellulose with manure by comparing the first-order equation, including in the equation the latency time (13) and the modified Gompertz equation. They concluded that both models did not offer significant differences in the coefficient of determination obtained in the models (r^2),

neither in the methane potential predicted *Me* nor between the constant kinetics *k* and $v_{M\max}$. However, it shows that the first-order kinetic model provides a longer latency time. The maximum methane potential *Me* was between 0.30 and 0.33 m^3/kg SV:

$$M = M_e \cdot \left(1 - e^{-k \cdot \left(t - t_{lag}\right)}\right) \tag{13}$$

Zhang et al. [34] also compared the modified Gompertz equation and thefirst-order kinetic model according to Eq. (13). Zhang confirms that the first-order kinetic model provides longer latency times and methane potentials than Gompertz. However, it provides slightly lower coefficients of determination.

4.2 Two-step reaction with first-order kinetics

Shin and Song [35] considered anaerobic digestion as a two-step process that could work at different speeds. Although this comprises a complex hydrolytic, acetogenic, and methanogenic process, a more suitable kinetic model than the previous one would consist in first considering the formation of volatile fatty acids (*VFAs*) from the substrate *Se* and, subsequently, the conversion of these acids into methane (*M*).

The formation of volatile fatty acids depends on the substrate concentration, following first-order kinetics, where k_1 is the kinetic constant of transformation of the substrate to *VFA, S* is the substrate concentration, and S_{VFA} is the concentration of acid grades:

$$\frac{dS_{VFA}}{dt} = k_1 \cdot S$$

Given the $S = S_0 \cdot e^{-k_1 \cdot t}$, you have the equation:

$$\frac{dS_{VFA}}{dt} = k_1 \cdot S_0 \cdot e^{-k_1 \cdot t}$$

On the other hand, the elimination of the fatty acids will depend on the concentration of the same, also following first-order kinetics, being k_2 as the kinetic constant of transformation of the *VFA* to *M*.

According to the mass balance in the formation of the *VFA*, a differential equation of constant coefficients of first order (14) is obtained:

$$\frac{dS_{VFA}}{dt} = k_1 \cdot S_0 \cdot e^{-k_1 \cdot t} - k_2 \cdot S_{VFA}$$
$$\frac{dS_{VFA}}{dt} + k_2 \cdot S_{VFA} = k_1 \cdot S_0 \cdot e^{-k_1 \cdot t} \tag{14}$$

such as

$$y' + a(x) \cdot y = b(x)$$
$$y = e^{-\int a(x)dx} \cdot \int b(x) \cdot e^{\int a(x)dx} dx + C \cdot e^{-\int a(x)dx}$$

The solution to Eq. (14) results

$$S_{VFA} = k_1 \cdot S_0 \cdot \frac{e^{-k_2 \cdot t} - e^{-k_1 \cdot t}}{k_2 - k_1}$$

From this equation, the accumulated methane production is obtained as

$$\frac{dM}{dt} = k_2 \cdot S_{VFA}$$

$$\frac{dM}{dt} = k_2 \cdot k_1 \cdot S_0 \cdot \frac{e^{-k_2 \cdot t} - e^{-k_1 \cdot t}}{k_2 - k_1}$$

$$M = S_0 \cdot \left(1 - \frac{k_1 e^{-k_2 \cdot t} - k_2 e^{-k_1 \cdot t}}{k_1 - k_2}\right)$$

4.3 Reaction in two speeds of a single step with first-order kinetics

The chemical composition of the substrates is generally heterogeneous and can be constituted by several fractions with different hydrolysis rates. This implies that we can consider the process as two parallel but independent mechanisms that occur simultaneously. If we define α as the relation between the amount of rapidly degradable substrate and the total a, k_F as the first-order kinetic constant for degradation of rapidly degradable substrate, and k_L as the first-order kinetic constant for the degradation of slowly degradable substrate, the amount of methane produced can be defined with the model used by Kusch et al. [36] or Luna del Risco [37]:

$$M = S_e \cdot \left(1 - \alpha \cdot e^{-k_F \cdot t} - (1 - \alpha) \cdot e^{-k_L \cdot t}\right)$$

Dennehy et al. [15] compared three different kinetic models to determine the most suitable to describe the kinetics of the discontinuous co-digestion of food waste and pig manure at 37°C: (1) first order, (2) Gompertz, and (3) two-speed one-step reaction with first-order kinetics. They showed that the three models provide similar determination coefficients; however, the RMSE (root of the mean of the squares of the errors) is significantly reduced when the two-speed digestion is considered. The worst RMSE was for the Gompertz model. The first-order kinetic model reduced the RMSE by 39%, and the first-order kinetic model with two speeds reduced the RMSE by 80%. The highest methane yields they obtained were 0.521 ± 29 m^3 CH4 kg^{-1} VS.

4.4 Reaction in two speeds of two steps with first-order kinetics

If we consider two steps in each of the fractions of which the substrate is composed, both for the rapidly degradable substrate fraction and for the slowly degradable substrate fraction, we can obtain the following equation:

$$M = S_e \cdot \left[\alpha \cdot \left(1 - \frac{k_{HF} e^{-k_{MF} \cdot t} - k_{MF} e^{-k_{HF} \cdot t}}{k_{HF} - k_{MF}}\right) + (1 - \alpha) \cdot \left(1 - \frac{k_{HL} e^{-k_{ML} \cdot t} - k_{ML} e^{-k_{HL} \cdot t}}{k_{HL} - k_{ML}}\right)\right]$$

Brulé et al. [31] evaluated the four kinetic models described, concluding that the models that consider an easy speed in both a step and two steps yield a reasonable estimate. In contrast, the model that considers two speeds with a single step produces overestimates. Therefore, it is considered inadequate. This overestimation is corrected by applying the two-step model at two speeds but complicates its application.

5. Model based on the transfer function

Several studies, such as Ghufran and Charles [38], Li et al. [39], or Zahan et al. [13], have used a function derived from the first-order kinetic model but which substitutes the kinetic constant for the ratio between the maximum and the methane velocity:

$$M = M_e \cdot \left(1 - e^{-k \cdot \left(t - t_{lag}\right)}\right)$$

$$M = M_e \cdot \left(1 - e^{-\frac{v_{\max M}}{M_e} \cdot \left(t - t_{lag}\right)}\right)$$

6. Cone model

On the other hand, researchers, such as Pitt et al. [40], El-Mashad [41], Li et al. [39], and Zahan et al. [13], analyzed the cone model. This model describes the fermentation according to Eq. (15):

$$M = \frac{M_e}{1 + (k \cdot t)^{-n}} \tag{15}$$

7. Comparison of models

For the evaluation of the models, most researchers usually use two statistics: (a) coefficient of determination of the fit (r^2) and (b) root of the mean of the squares of the errors (RMSE) calculated by Eq. (16), where M_{model} is the value of methane predicted by the model at an instant t and M_{ob} is the value of methane observed experimentally:

$$RMSE = \sqrt{\frac{\sum (M_{\text{model}} - M_{\text{ob}})^2}{n}} \tag{16}$$

Pitt et al. [40], Ghufran and Charles [38], El-Mashad [41], Li et al. [39], and Zahan et al. [13] compared the modified Gompertz model, the first-order kinetic model, the transfer function model, and the cone model, for different types of substrates and combinations in co-digestion.

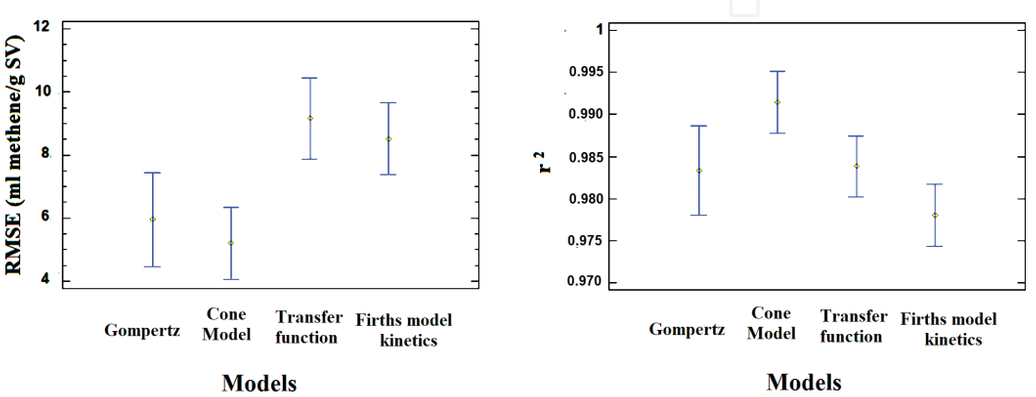

Figure 2.
LSD intervals of the analysis of variance at 95% confidence level for the comparison of the RMSE and the r^2 of the different models applied to the fermentation of different substances and combinations in co-digestion.

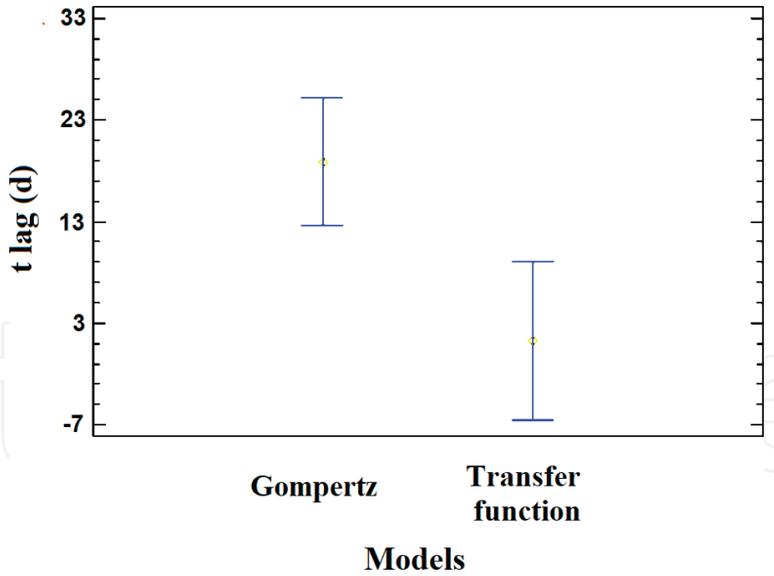

Figure 3.
LSD intervals of the analysis of variance at 95% confidence level for the comparison of the latency time of the different models applied to the fermentation of different substances and combinations in co-digestion.

Comparing the values of r^2, RMSE, and lag time provided by analysis of variance, the results shown in **Figures 2** and **3** were obtained.

As you can see, all the models provide high coefficients of determination, and there are few differences between them. The transfer model and the first-order kinetic model generally produce higher RMSE, so the modified Gompertz model and the cone model make more accurate estimates. However, the Gompertz model estimates higher latency periods.

8. Conclusion

In this research work, the most important kinetic models used to describe anaerobic fermentation have been developed. The comparison between them is a subject currently studied as demonstrated in recent publications. All of them provide high coefficients of determination; however, they present significant differences in the RMSE.

The production of methane in most cases ranges between 0.15 and 0.65 $m^3\ kg^{-1}SV$, under mesophilic conditions (30–37°C). However, digestion processes can be classified into three groups according to the methane production potential:

a. low-production processes, when the amount of methane produced is between 0.15 and 0.30 $m^3\ kg^{-1}SV$.

b. medium-production processes, when the amount of methane produced is between 0.30 and 0.45 $m^3\ kg^{-1}SV$.

c. high-production processes, when the amount of methane produced is greater than 0.45 $m^3\ kg^{-1}SV$.

The average lag time is 14 days.
The mean of the first-order kinetic constant is 0.11 d^{-1}.

Author details

Borja Velázquez-Martí[1*], Orlando W. Meneses-Quelal[1], Juan Gaibor-Chavez[2] and Zulay Niño-Ruiz[2]

1 Departamento de Ingeniería Rural y Agroalimentaria, Universitat Politècnica de Valencia, Valencia, Spain

2 Departamento de Investigación, Centro de Investigación del Ambiente, Universidad Estatal de Bolívar, Guaranda, Ecuador

*Address all correspondence to: borvemar@dmta.upv.es

References

[1] Deublein D, Steinhauser A. Biogas from Waste and Renewable Resources: An Introduction. 2nd ed. Weinheim, Germany: Wiley-VCH Verlag GmbH & Co. KGaA; 2010. 532 p. DOI: 10.1002/9783527632794

[2] Chynoweth DP, Wilkie AC, Owens JM. Anaerobic processing of piggery wastes: A review. In: ASAE Annual International Meeting; 12–16 July. Orlando, Florida, USA: St Joseph: American Society of Agricultural Engineers (ASAE); 1998. 38 pp

[3] Capson-Tojo G, Rouez M, Crest M, Trably E, Steyer J-P, Bernet N, et al. Kinetic study of dry anaerobic co-digestion of food waste and cardboard for methane production. Waste Management. 2017;**69**:470-479. DOI: 10.1016/j.wasman.2017.09.002

[4] Bayrakdar A, Sürmeli RÖ, Çalli B. Anaerobic digestion of chicken manure by a leach-bed process coupled with side-stream membrane ammonia separation. Bioresource Technology. 2018;**258**:41-47. DOI: 10.1016/j.biortech.2018.02.117

[5] Franco RT, Buffière P, Bayard R. Co-ensiling of cattle manure before biogas production: Effects of fermentation stimulants and inhibitors on biomass and methane preservation. Renewable Energy. 2018;**121**:315-323. DOI: 10.1016/j.renene.2018.01.035

[6] Guo J, Cui X, Sun H, Zhao Q, Wen X, Pang C, et al. Effect of glucose and cellulase addition on wet-storage of excessively wilted maize stover and biogas production. Bioresource Technology. 2018;**259**:198-206. DOI: 10.1016/j.biortech.2018.03.041

[7] Li W, Siddhu MAH, Amin FR, He Y, Zhang R, Liu G, et al. Methane production through anaerobic co-digestion of sheep dung and waste paper. Energy Conversion and Management. 2018;**156**:279-287. DOI: 10.1016/j.enconman.2017.08.002

[8] Mancini G, Papirio S, Lens PNL, Esposito G. Increased biogas production from wheat straw by chemical pretreatments. Renewable Energy. 2018;**119**:608-614. DOI: 10.1016/j.renene.2017.12.045

[9] Martín Juárez J, Riol Pastor E, Fernández Sevilla JM, Muñoz Torre R, García-Encina PA, Bolado Rodríguez S. Effect of pretreatments on biogas production from microalgae biomass grown in pig manure treatment plants. Bioresource Technology. 2018;**257**:30-38. DOI: 10.1016/j.biortech.2018.02.063

[10] Mustafa AM, Li H, Radwan AA, Sheng K, Chen X. Effect of hydrothermal and $Ca(OH)_2$ pretreatments on anaerobic digestion of sugarcane bagasse for biogas production. Bioresource Technology. 2018;**259**:54-60. DOI: 10.1016/j.biortech.2018.03.028

[11] Vazifehkhoran AH, Shin SG, Triolo JM. Use of tannery wastewater as an alternative substrate and a pre-treatment medium for biogas production. Bioresource Technology. 2018;**258**:64-69. DOI: 10.1016/j.biortech.2018.02.116

[12] Xu W, Fu S, Yang Z, Lu J, Guo R. Improved methane production from corn straw by microaerobic pretreatment with a pure bacteria system. Bioresource Technology. 2018;**259**:18-23. DOI: 10.1016/j.biortech.2018.02.046

[13] Zahan Z, Othman MZ, Muster TH. Anaerobic digestion/co-digestion kinetic potentials of different agro-industrial wastes: A comparative batch

study for C/N optimisation. Waste Management. 2018;**71**:663-674. DOI: 10.1016/j.wasman.2017.08.014

[14] Aboudi K, Álvarez-Gallego CJ, Romero-García LI. Evaluation of methane generation and process stability from anaerobic co-digestion of sugar beet by-product and cow manure. Journal of Bioscience and Bioengineering. 2016;**121**(5):566-572. DOI: 10.1016/j.jbiosc.2015.10.005

[15] Dennehy C, Lawlor PG, Croize T, Jiang Y, Morrison L, Gardiner GE, et al. Synergism and effect of high initial volatile fatty acid concentrations during food waste and pig manure anaerobic co-digestion. Waste Management. 2016; **56**:173-180. DOI: 10.1016/j.wasman. 2016.06.032

[16] Glanpracha N, Annachhatre AP. Anaerobic co-digestion of cyanide containing cassava pulp with pig manure. Bioresource Technology. 2016; **214**:112-121. DOI: 10.1016/j.biortech. 2016.04.079

[17] Marin Batista J, Salazar L, Castro L, Escalante-Hernández H. Co-digestión anaerobia de vinaza y gallinaza de jaula: alternativa para el manejo de residuos agrícolas colombianos. Revista Colombiana de Biotecnología. 2016; **18**(2):6-12. Retrieved from: https:// dialnet.unirioja.es/descarga/articulo/ 5798936.pdf

[18] Aboudi K, Álvarez-Gallego CJ, Romero-García LI. Semi-continuous anaerobic co-digestion of sugar beet byproduct and pig manure: Effect of the organic loading rate (OLR) on process performance. Bioresource Technology. 2015;**194**:283-290. DOI: 10.1016/j. biortech.2015.07.031

[19] Belle AJ, Lansing S, Mulbry W, Weil RR. Anaerobic co-digestion of forage radish and dairy manure in complete mix digesters. Bioresource Technology. 2015;**178**:230-237. DOI: 10.1016/j. biortech.2014.09.036

[20] Cestonaro T, Costa MSS de M, Costa LA de M, Rozatti MAT, Pereira DC, Francisconi Lorin HE, et al. The anaerobic co-digestion of sheep bedding and ⩾50% cattle manure increases biogas production and improves biofertilizer quality. Waste Management. 2015;**46**:612-618. DOI: 10.1016/j.wasman.2015.08.040

[21] Di Maria F, Sordi A, Cirulli G, Micale C. Amount of energy recoverable from an existing sludge digester with the co-digestion with fruit and vegetable waste at reduced retention time. Applied Energy. 2015; **150**:9-14. DOI: 10.1016/j.apenergy. 2015.01.146

[22] Fu SF, Wang F, Yuan XZ, Yang ZM, Luo SJ, Wang CS, et al. The thermophilic (55°C) microaerobic pretreatment of corn straw for anaerobic digestion. Bioresource Technology. 2015;**175**:203-208. DOI: 10.1016/j.biortech.2014.10.072

[23] Fu SF, Shi XS, Xu XH, Wang CS, Wang L, Dai M, et al. Secondary thermophilic microaerobic treatment in the anaerobic digestion of corn straw. Bioresource Technology. 2015;**186**: 321-324. DOI: 10.1016/j.biortech. 2015.03.053

[24] Agyeman FO, Tao W. Anaerobic co-digestion of food waste and dairy manure: Effects of food waste particle size and organic loading rate. Journal of Environmental Management. 2014;**133**: 268-274. DOI: 10.1016/j.jenvman. 2013.12.016

[25] Velázquez-Martí B. Aprovechamieno de la biomasa para uso energético. 1st ed. Barcelona, Spain: Reverté; 2017. 840 p. ISBN: 9788429147544

[26] Winsor CP. The Gompertz curve as a growth curve. Proceedings of the National Academy of Sciences. 1932;**18**: 1-8

[27] Gompertz B. On the nature of the function expressive of the law of human mortality, and on a new mode on determining the value of live contingencies. Philosophical Transactions of the Royal Society of London. 1825;**115**:513-585

[28] Zwietering MH, Jongenburger I, Rombouts FM, van't Riet K. Modeling of the bacterial growth curve. Applied and Environmental Microbiology. 1990; **56**(6):1875-1881

[29] Bah H, Zhang W, Wu S, Qi D, Kizito S, Dong R. Evaluation of batch anaerobic co-digestion of palm pressed fiber and cattle manure under mesophilic conditions. Waste Management. 2014;**34**(11):1984-1991. DOI: 10.1016/j.wasman.2014.07.015

[30] Lay JJ, Li YY, Noike T. Effect of moisture content and chemical nature on methane fermentation characteristics of municipal solid wastes. Doboku Gakkai Ronbunshu. 1996;**1996**(552): 101-108. DOI: 10.2208/jscej.1996.552_101

[31] Brulé M, Oechsner H, Jungbluth T. Exponential model describing methane production kinetics in batch anaerobic digestion: A tool for evaluation of biochemical methane potential assays. Bioprocess and Biosystems Engineering. 2014;**37**(9):1759-1770. DOI: 10.1007/s00449-014-1150-4

[32] Angelidaki I, Alves M, Bolzonella D, Borzacconi L, Campos JL, Guwy AJ, et al. Defining the biomethane potential (BMP) of solid organic wastes and energy crops. A proposed protocol for batch assays. Water Science and Technology. 2009;**59**(5):927-934. Retrieved from http.//wst.iwaponline.com/content/59/5/927.abstract

[33] Díaz I, Donoso-Bravo A, Fdz-Polanco M. Effect of microaerobic conditions on the degradation kinetics of cellulose. Bioresource Technology. 2011;**102**(21):10139-10142. DOI: 10.1016/j.biortech.2011.07.096

[34] Zhang H, Luo L, Li W, Wang X, Sun Y, Sun Y, et al. Optimization of mixing ratio of ammoniated rice straw and food waste co-digestion and impact o f trace element supplementation on biogas production. Journal of Material Cycles and Waste Management. 2018;**20**(2): 745-753. DOI: 10.1007/s10163-017-0634-0

[35] Shin HS, Song YC. A model for evaluation of anaerobic degradation characteristics of organic waste: Focusing on kinetics, rate-limiting step. Environmental Technology. 1995;**16**:775-784. DOI: 10.1080/09593331608616316

[36] Kusch S, Oechsner H, Jungbluth T. Biogas production with horse dung in solid-phase digestion systems. Bioresource Technology. 2008;**99**: 1280-1292. DOI: 10.1016/j.biortech.2007.02.008

[37] Luna del Risco M, Normak A, Orupold K. Biochemical methane potential of different organic wastes and energy crops from Estonia. Agronomy Research. 2011;**9**:331-342

[38] Ghufran R, Charles B. The use of a specific function to estimate maximum methane production in a batch-fed anaerobic reactor. Journal of Chemical Technology and Biotechnology. 2004; **79**(10):1174-1178. DOI: 10.1002/jctb.1107

[39] Li K, Liu R, Sun C. Comparison of anaerobic digestion characteristics and kinetics of four livestock manures with different substrate concentrations. Bioresource Technology. 2015;**198**: 133-140. DOI: 10.1016/j.biortech.2015.08.151

[40] Pitt RE, Cross TL, Pell AN, Schofield P, Doane PH. Use of in vitro gas production models in ruminal kinetics. Mathematical Biosciences.

1999;**159**(2):145-163. DOI: 10.1016/S0025-5564(99)00020-6

[41] El-Mashad HM. Kinetics of methane production from the codigestion of switchgrass and Spirulina platensis algae. Bioresource Technology. 2013; **132**:305-312. DOI: 10.1016/j.biortech.2012.12.183